RESEARCH ARTICLES

Chaotic dynamics of some quantum anharmonic oscillators

P. K. Chattaraj*, S. Sengupta and A. Poddar

Department of Chemistry, Indian Institute of Technology, Kharagpur 721 302, India

Quantum domain behaviour of classically chaotic systems is studied using the quantum theory of motion in the sense of classical interpretation of quantum mechanics as developed by de Broglie and Bohm. Dynamics of quantum Hénon–Heiles oscillator, Barbanis oscillator and CTW oscillator are analysed with the help of quantum Lyapunov exponent and Kolmogorov–Sinai entropy defined in terms of the distance between two initially close Bohmian trajectories. Standard diagnostics of quantum chaos like autocorrelation function and the associated power spectrum, nearest-neighbour spacing distribution, phase space volume, spectral rigidity, etc. support these results. Quantum theory of motion provides an alternative route for understanding quantum chaos. Nonlinear dynamics of integrable systems in quantum domain is also properly taken care of within this framework.

Of late, the quantum domain behaviour of classically chaotic systems has seen a great upsurge of interest[1–4]. Quantum dynamics of anharmonic oscillators like Hénon–Heiles system has been studied[5–19] extensively for this purpose. Wave packet dynamics[1–23] has been shown to be appropriate in analysing quantum manifestations of classical regular or chaotic dynamics. Various quantities

which reveal the signatures of chaotic behaviour of a quantum system can be calculated once the wave packet, $\psi(r, t)$, is obtained at different time steps as a solution to the pertinent time-dependent Schrödinger's equation (TDSE), viz.

$$\left[-\frac{\hbar^2}{2m} \left(\frac{\partial^2}{\partial x^2} + \frac{\partial^2}{\partial y^2} \right) + V \right] \Psi = i\hbar \frac{\partial \Psi}{\partial t}, \quad (1)$$

where the potential V for a generalized Hénon–Heiles system takes the following form,

$$V(x, y) = \frac{1}{2}(Ax^2 + By^2) + \lambda \left(Cx^2 y + \frac{D}{3} y^3 \right). \quad (2)$$

In eq. (2) λ is a parameter which measures the degree of nonlinearity and nonintegrability and may be treated as a time-like quantity[24,25]. In the conventional Hénon–Heiles potential $\lambda = A = B = C = 1$ and $D = -1$. However, it is not sacrosanct that one has to resort to the value of λ as unity only. In fact one can either take $\lambda = 1$ and vary $\hbar$, or set $\hbar = 1$ and vary λ to obtain similar results, viz. the system in higher energy levels exhibiting

*For correspondence. (e-mail: pkcj@hijli.iitkgp.ernet.in)

chaos while lower energy levels are similar to those of independent harmonic oscillators[3]. This problem involves two parameters, λ and $\hbar$. While λ is a classical parameter of nonlinearity, $\hbar$ takes care of the quantum aspects. In the classical limit, $\hbar$ goes to zero and in this limit one recovers the classical regular or chaotic behaviour of the corresponding quantum system. But one cannot vary $\hbar$ and λ simultaneously because the generalized Hénon–Heiles Hamiltonian needs three physical constants, viz. mass, frequency and length in order that it represents a real nonlinear system[3]. Hence, the parameter λ now fixes the length scale as it varies inversely with length and it no longer provides the strength of nonlinear coupling between the motions along x and y directions. Oscillators having the same generalized potential form (eq. 2), which have been studied for various purposes, include a) Harmonic oscillator: $A = B = 1$, $\lambda = 0$; b) Hénon–Heiles oscillator: $\lambda \neq 0$, $A = B = C = 1$ and $D = -1$; c) Barbanis oscillator[26]: $\lambda \neq 0$, $A = B = C = 1$ and $D = 0$, and d) Chang–Tabor–Weiss (CTW) oscillator[27]: $\lambda \neq 0$, $A = C = 1$, $B = D = 16$. It may be noted that a is linear, b and c are both nonlinear and nonintegrable and d is nonlinear but integrable. Making use of $\Psi(r, t)$ from eq. (1), chaotic dynamics of a Hénon–Heiles system has been analysed[6] in terms of phase space trajectories, autocorrelation function and the associated power spectrum as well as the volume of the phase space. Short- and long-range correlations have also been studied[28] via the behaviour of nearest-neighbour spacing distribution, $P(s)$, and spectral rigidity[29], Δ_3. Another recently developed approach of analysing quantum chaos is through quantum theory of motion (QTM)[30] in the spirit of the causal interpretation of quantum mechanics as introduced by de Broglie[31] and Bohm[32]. Quantum fluid dynamics (QFD) of Madelung[33] has also been used for this purpose[16–18]. Quantum standard map[34], Weigert's quantum cat map[35], Rydberg atoms in external fields[36] and a quantum Hénon–Heiles oscillator[19] have been studied successfully using QTM. Quantities calculated for this purpose are[19,34,35] – phase space distance function and the associated Kolmogorov–Sinai (KS) entropy, de Broglie wavelength and a return map. To our knowledge QTM has been used for the first time in the current work in analysing the quantum domain behaviour of a nonlinear integrable oscillator. This study may suggest whether QTM can be applied in understanding the nature of 'quantum solitons'.

In the present paper we study the dynamics of four types of quantum oscillators mentioned above (cases a–d) in terms of QTM. For comparison we also calculate survival probability (autocorrelation function) and the corresponding power spectrum, phase space volume, nearest-neighbour spacing distribution (NNSD) and spectral rigidity. Theoretical background of the present work is presented in Section 1 while Section 2 describes the

necessary numerical details. Section 3 contains the results and discussion. The salient features of the present study are summarized in Section 4.

1. Theoretical background

In quantum theory of motion the complete description of a physical system involves both wave and particle pictures. The wave motion is governed by the solution of the TDSE eq. (1). For a given initial position, the motion of a point particle guided by this wave is represented by the velocity

$$r = \frac{1}{m} \nabla S(r, t)|_{r = r(t)}, \tag{3}$$

where S is the phase of the wave function as appeared in its polar form as follows:

$$\Psi(r, t) = R(r, t) \exp[iS(r, t)/\hbar]. \tag{4}$$

Now, an ensemble of particle motions guided by the same wave can be constructed by varying initial positions in such a way that the probability of the particle being in this ensemble between r and $r + dr$ at time t is given by[30] $\rho(r, t) dr$, where $\rho(r, t)$ is $|\Psi(r, t)|^2$. Solution of eq. (3) with various initial positions would yield the so-called 'Bohmian trajectories'. In order to study the quantum signature of chaos through sensitive dependence on initial condition a phase space distance function[19,34,35] can be defined as

$$D(t) = [(x_1(t) - x_2(t))^2 + (y_1(t) - y_2(t))^2$$

$$+ (p_{x_1}(t) - p_{x_2}(t))^2 + (p_{y_1}(t) - p_{y_2}(t))^2]^{1/2}, \tag{5}$$

where (x, p_x, y, p_y) refer to a point in phase space.

A generalized quantum Lyapunov exponent can also be defined as follows[34,35] in the same spirit as in classical dynamics,

$$\Lambda = \lim_{\substack{D(t) \to 0 \\ t \to \infty}} \frac{1}{t} \ln[D(t)/D(0)]. \tag{6}$$

Corresponding KS entropy has also been defined as[34,35]

$$H = \sum_{\Lambda_i > 0} \Lambda_i. \tag{7}$$

It has been stated that[34], 'Quantum dynamics is chaotic, if in a given region of phase space the flow of trajectories, according to the Hamilton–Jacobi formulation of quantum mechanics, has positive KS entropy'.

Other well-known quantities used to identify chaos and analysed in the present work are now briefly mentioned. Autocorrelation function is given as[6,20]

$$C(t) = |\langle \Psi(r, 0) | \Psi(r, t) \rangle|, \qquad (8)$$

and the corresponding power spectrum is obtained as the following Fourier transform:

$$I(E) = \left| \frac{1}{\tau} \int_0^\tau C(t) \, e^{iEt/\hbar} \, dt \right|^2. \qquad (9)$$

Sharp decay of $C(t)$ and existence of many closely-spaced lines in its power spectrum generally signal a chaotic dynamics[3].

Phase space volume is defined as[6]

$$V_{ps}(t) = [\langle(x - \langle x\rangle)^2\rangle \langle(p_x - \langle p_x\rangle)^2\rangle \langle(y - \langle y\rangle)^2\rangle$$

$$\times \langle(p_y - \langle p_y\rangle)^2\rangle]^{1/2}. \qquad (10)$$

A sharp increase in $V_{ps}(t)$ implies chaotic motion[6]. This quantity is same as the associated uncertainty product which can be used as a measure of quantum fluctuations[37]. Classical chaos generally enhances quantum fluctuations[6,37].

Quantum domain behaviour of classically chaotic systems is studied in terms of short-range and long-range correlations of the eigenvalues[23,28,29]. For study of the short-range correlations, generally nearest-neighbour spacing distribution, $P(s)$ is used as a diagnostic. For a classically chaotic system the level statistics is Wigner in nature[3], i.e.,

$$P_w(s) = \frac{\pi s}{2} \exp\left(\frac{-\pi s^2}{4}\right), \qquad (11)$$

while a Poisson distribution is obtained for the corresponding integrable counterpart[3], viz.

$$P_p(s) = \exp(-s) \qquad (12)$$

where s is the gap between the two nearest energy levels properly normalized in order to have uniform[38] mean density of those levels[23,38]. On the other hand, the long-range correlation[3] is understood in terms of the spectral rigidity, $\Delta_3(L)$ for an energy interval L. For a system exhibiting chaos in the classical domain, a Gaussian orthogonal ensemble (GOE) represents the corresponding Δ_3 behaviour[3]

$$\Delta_3^{GOE}(L) = \frac{1}{\pi^2} \log(L) - 0.00695, \qquad (13)$$

while Poisson behaviour is observed for the classically integrable systems,

$$\Delta_3^P(L) = \frac{L}{15}. \qquad (14)$$

2. Numerical solution

The numerical solution starts with the propagation of a Gaussian wavepacket under the influence of the potential corresponding to a given oscillator. For this purpose the pertinent TDSE eq. (1) is solved to monitor the temporal evolution of $\Psi(r, t)$ using a Peaceman–Rachford type finite difference algorithm[39]. The formal solution to TDSE eq. (1) can be written as[39]

$$\Psi(x, y, t) = \exp(-i\hat{H}\Delta t) \, \Psi(x, y, t = 0), \qquad (15)$$

where $\hat{H}$ is the Hamiltonian operator and $\hbar = 2m = 1$. The Cayley form of the unitary approximation to eq. (15) can be written as[39]

$$(1 - i\delta x^2/\varepsilon) \, \Phi_{l,m}^n = (1 + i\delta y^2/\varepsilon) \, \Psi_{l,m}^n, \qquad (16)$$

where $1 \le l \le L$, $1 \le m \le M$, $\Psi_{l,m}^n = \Psi((l-1)\Delta x, (m-1)\Delta y, n\Delta t)$, $\varepsilon = 2\Delta x^2/\Delta t$, Φ is an intermediate function and δx^2 and δy^2 are central difference operators in x and y directions respectively[39]. The details of the numerical technique are available elsewhere[39]. The numerical algorithm used here is stable[40] because of the presence of $i = \sqrt{-1}$. As a further check of the numerical accuracy of the scheme we have verified the conservation of the norm and the energy as well as the reproduction of the initial wave packet through forward propagation up to the end of the simulation followed by back evolution[6].

The boundary conditions for this problem are as follows

$$\Psi(\pm\infty, y, t) = 0 \qquad \supset y, t, \qquad (17a)$$

$$\Psi(x, \pm\infty, t) = 0 \qquad \supset x, t. \qquad (17b)$$

The initial condition, however, has been chosen depending on the problem concerned, viz. cases **a, b, c**:

$$\Psi(x, y, t = 0) = \left(\frac{1}{\pi\sqrt{2}}\right)^{1/2}$$

$$\times \exp\left(-\frac{1}{2\sqrt{2}}[(x - x_0)^2 + (y - y_0)^2]\right), \qquad (18a)$$

case **d**:

$$\Psi(x, y, t = 0) = \left(\frac{\sqrt{2}}{\pi}\right)^{1/2}$$

$$\times \exp\left(-\frac{1}{2\sqrt{2}}[(x - x_0)^2 + 4(y - y_0)^2]\right), \qquad (18b)$$

Mesh sizes adopted are $\Delta x = \Delta y = 0.1$, $\Delta t = 0.02$. Calculation is carried out for $-6 \leq x$, $y \leq 6$ and for 2.5×10^4 time steps.

Once we know $\Psi(x, y, t)$ we can rewrite eq. (3) as

$$\dot{\mathbf{r}} = \frac{1}{m} \nabla S(\mathbf{r}, t)\big|_{\mathbf{r}=\mathbf{r}(t)} = \mathrm{Re}\left[-\frac{i\hbar \nabla \Psi}{m\Psi} \right], \quad (19)$$

which can be solved with different initial conditions to obtain 'Bohmian trajectories'. Here we have used a second order Runge-Kutta method. While case **a** has zero λ value, for all other cases λ has been taken[6] as 0.1118034. Three initial positions[6] have been considered, viz. (1.36719, 1.36719) for cases **a** and **b** and (2.929688, 1.953125), (1.25, 0.5) for cases **c** and **d** respectively.

3. Results and discussion

Temporal behaviour of the distance function D is depicted in Figure 1. Unless otherwise specified, figures **a** to **d**

represent cases **a** to **d** respectively. Initial very small value of D does not change with time for the harmonic oscillator (case **a**). For the classically chaotic cases, viz. Hénon–Heiles (case **b**) and Barbanis (case **c**) oscillators D oscillates and becomes very large at times. It is heartening to note that the integrable CTW oscillator (case **d**) maintains its initial small value.

Figure 2 presents the associated KS entropies, H. As expected, H increases and then levels off to a small value for classically integrable cases (**a** and **d**) and increases abruptly to a large positive value for the classically chaotic cases (**b** and **c**). It is transparent from this study that two initially ($t = 0$) nearby 'Bohmian trajectories' remain close to each other for integrable cases and diverge rapidly in case of classically chaotic systems. Thus, QTM provides an alternative route in analysing 'quantum chaos', especially the quantum domain behaviour of a classically chaotic system. The QTM of the CTW system in the present study has confirmed that D and H do not exhibit any spurious nonlinear behaviour (cases **b** and **c**) as a numerical artifact as it does not show any chaotic signature in D
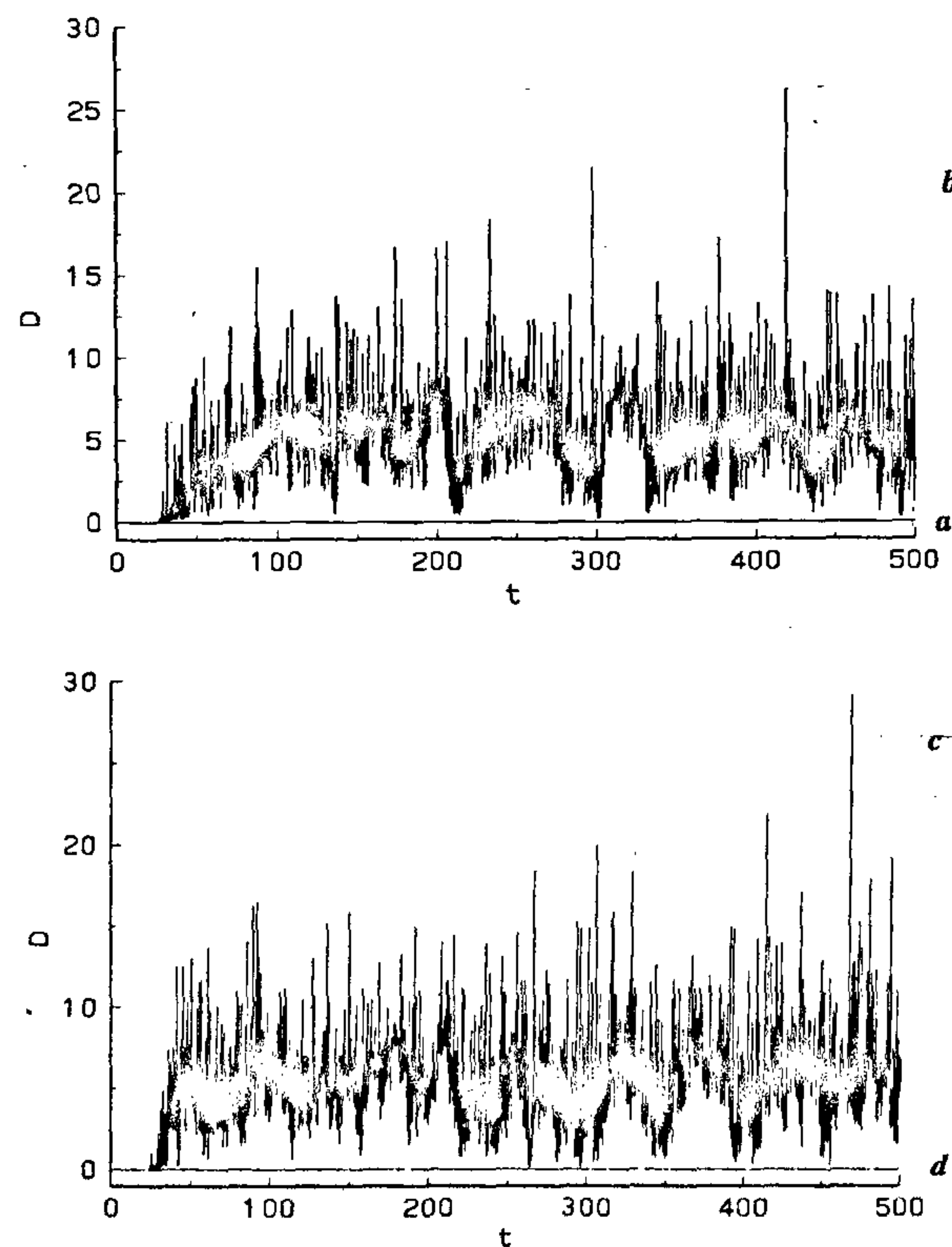

Figure 1. Time evolution of phase space distance, D for (a) harmonic oscillator with $x_0 = 1.36719$, $y_0 = 1.36719$, (b) Hénon–Heiles oscillator, with $\lambda = 0.1118034$ and $x_0 = 1.36719$, $y_0 = 1.36719$, (c) Barbanis oscillator, with $\lambda = 0.1118034$ and $x_0 = 2.929688$, $y_0 = 1.953125$, (d) CTW oscillator, $\lambda = 0.1118034$ and $x_0 = 1.25$, $y_0 = 0.5$. Figures a and b are presented together as is the case with Figures c and d.

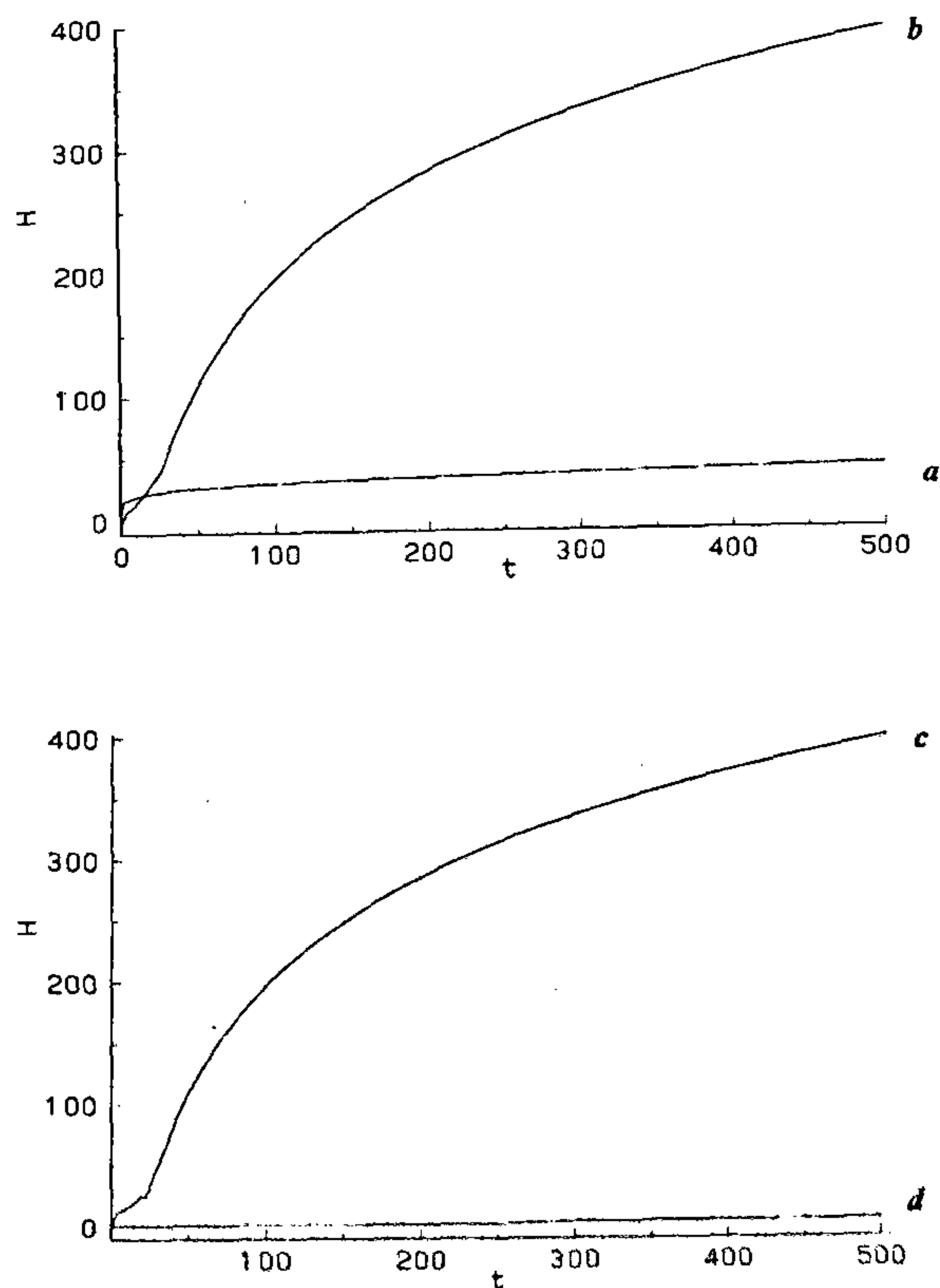**Figure 2.** Time evolution of KS entropy, H for cases a and b are presented together as is the case with Figures c and d.

and H for a highly nonlinear system whose actual dynamics is nonchaotic (case d). In Figures 1 and 2 we have demonstrated the temporal behaviour of D and H associated with the time development of an initial $(t = 0)$ Gaussian wavefunction. Recently two of us[36] have noticed in the context of the QTM study of quantum chaos in Rydberg atoms in an external oscillating electric field that the behaviour of D and H can differentiate between a regular and a chaotic system even in case a non-Gaussian initial wavefunction is used.

Autocorrelation functions, $C(t)$, and corresponding power spectra $I(E)$, are shown in Figures 3 and 4 respectively. Since the behaviour of any quantity in the two nonintegrable cases (b and c) is more or less similar as is also the case with the two integrable systems (a and d) we present one plot from each category (a and c) in Figures 3 to 5 although we comment on all four cases. For the cases a and d relatively high $C(t)$ values designate a high degree of correlation unlike in two other cases. Plots of $I(E)$ mimic this behaviour through a relatively simple spectra with a small number of lines in integrable cases and a large number of peaks in the nonintegrable cases.

In Figure 5 we present the phase space volume, V_{ps}. It clearly demonstrates that V_{ps} value remains small all

throughout for case a (and also d) but increases abruptly to a high value for case b (and also c). This behaviour is in conformity with that obtained by other workers in different contexts[37]. Thus classical chaos enhances quantum fluctuations.
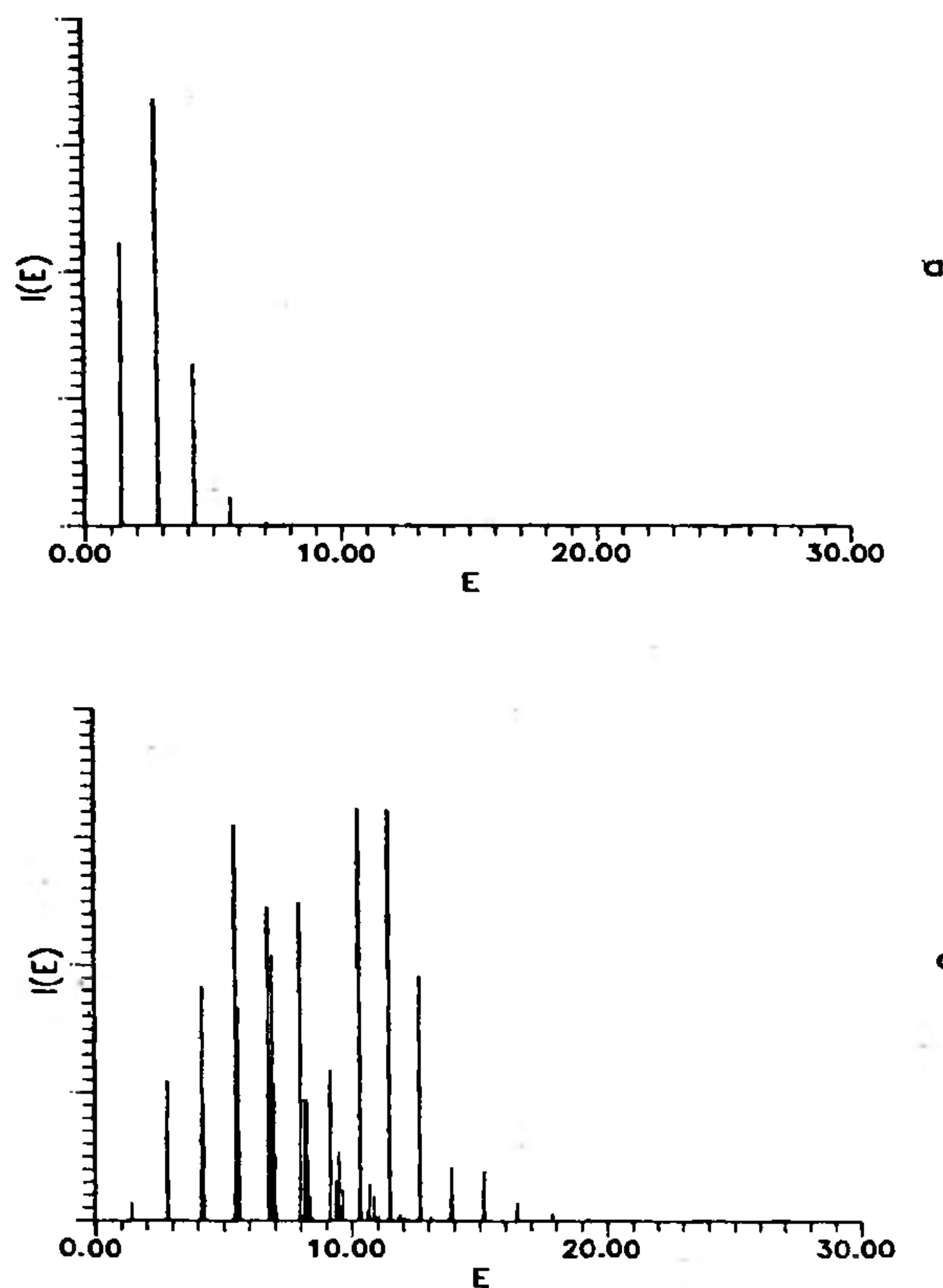
The nearest-neighbour spacing distribution, $P(s)$ is
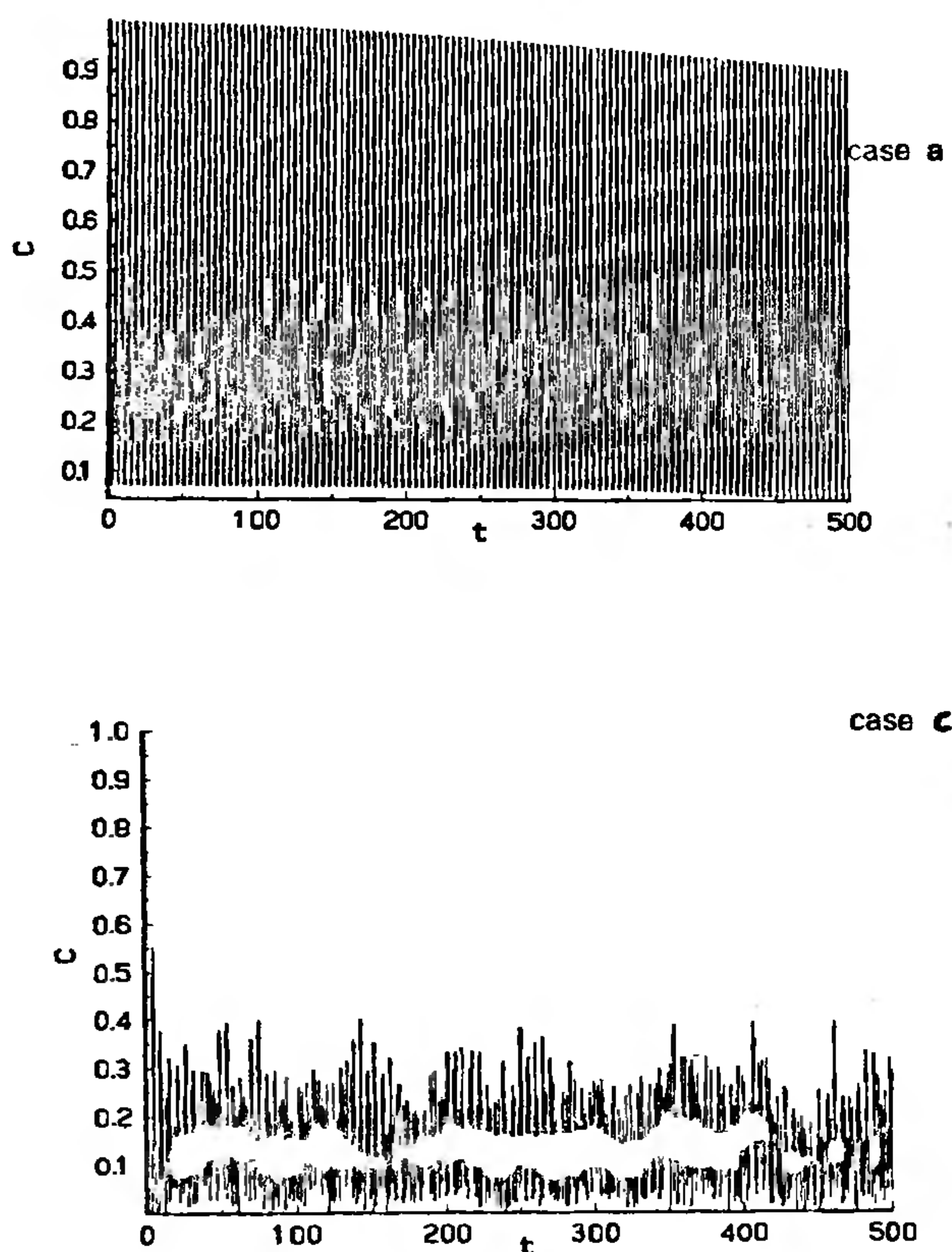
Figure 4. Power spectra, $I(E)$ for cases a and c.

Figure 3. Time evolution of autocorrelation, C for cases a and c.
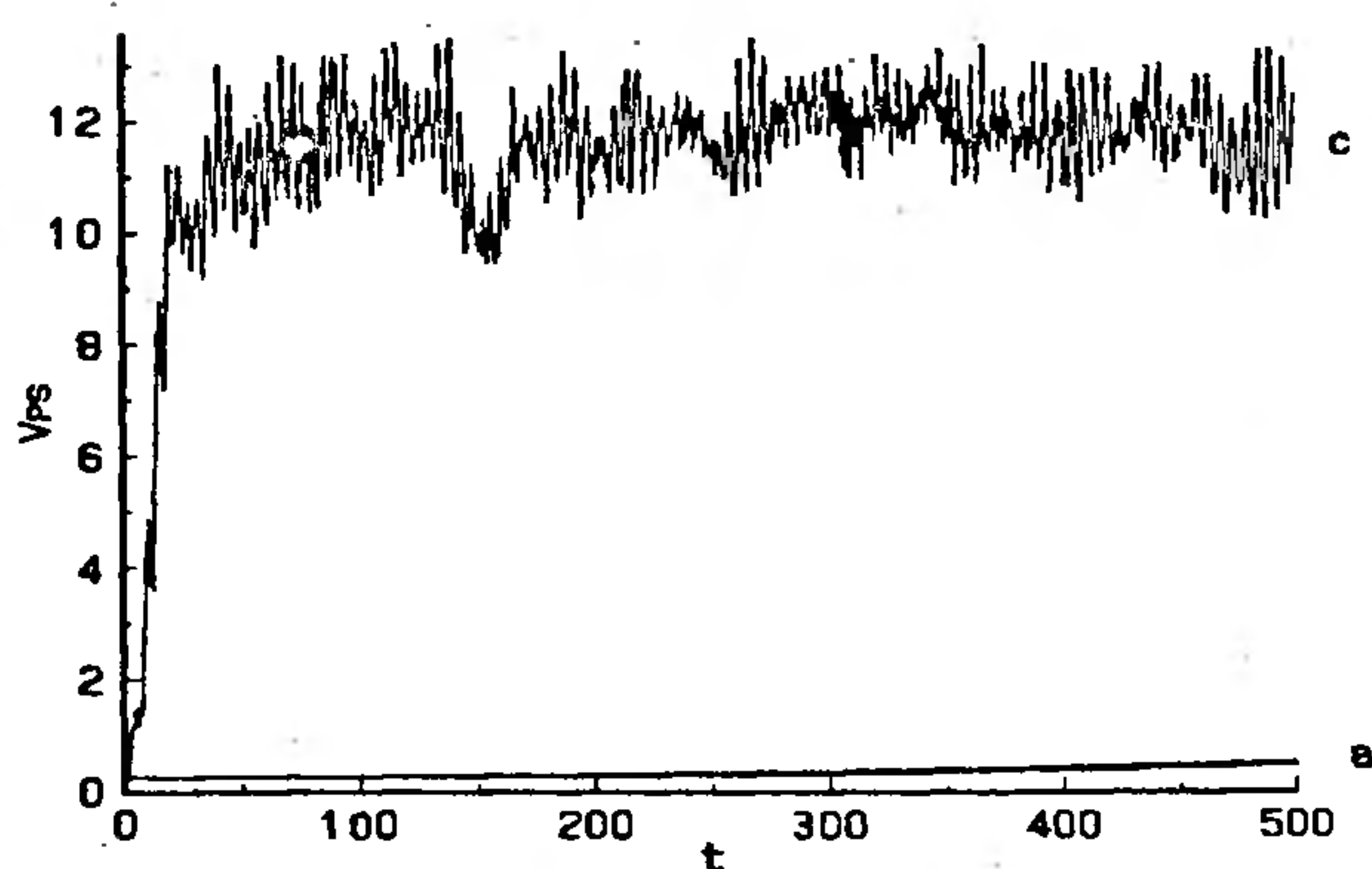
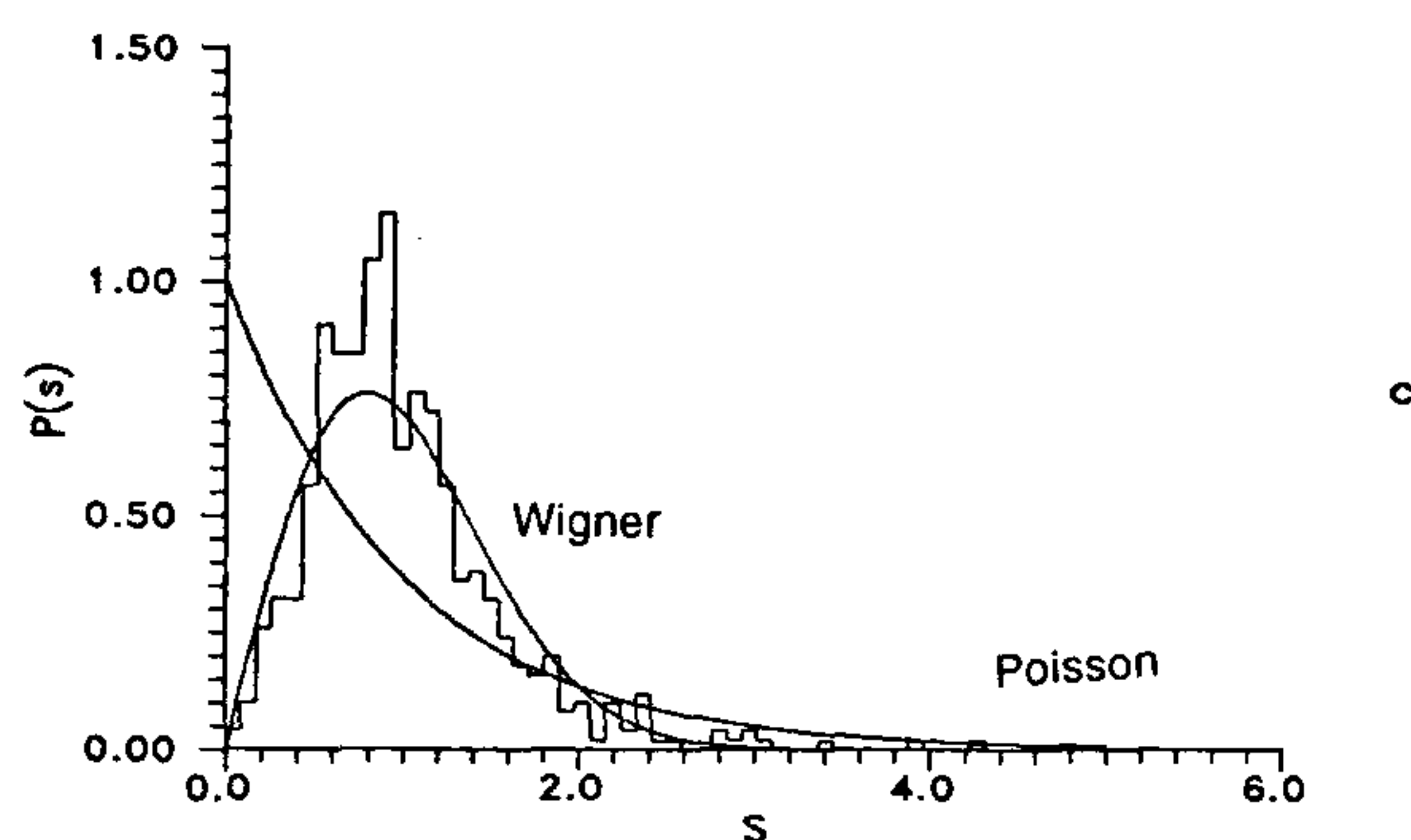Figure 5. Time evolution of phase space volume, V_{ps} for cases a and c.

Figure 6. Nearest-neighbour spacing distribution, $P(s)$ as a function of the spacing between consecutive energy levels s. Only case c is presented.

Figure 7. Spectral rigidity, $\Delta_3(L)$ as a function of energy interval L. Only case c is presented.

shown in Figure 6. For comparison we also plot the analytical Poisson and Wigner functions. Plots of $P(s)$ and $\Delta_3(L)$ for the integrable cases are not presented because they are standard and available elsewhere[28,29]. For two classically chaotic cases (b and c) the behaviour of $P(s)$ is more Wigner-like while cases a and d (not presented here), although integrable, do not exhibit a Poisson-like statistics, a fact already noticed by Berry and Tabor[41] for harmonic oscillators. It may be noted that a small number of energy levels in the integrable case also causes impediments towards a statistical analysis.

Figure 7 depicts the spectral rigidity, $\Delta_3(L)$ computed from the energy level spacings of the systems under consideration. The results are compared with the analytical Δ_3 curves for Poisson and Gaussian orthogonal ensembles (GOE). Classically chaotic cases (b and c) follow the analytical Δ_3 curve for GOE and hence bear the signatures of classical chaos in quantum domain. However, cases a and d (not presented here) for the integrable oscillators although markedly different from the other two cases do not exhibit any clear-cut Poisson-like distribution probably due to the small number of energy levels in these two cases.

4. Summary

Quantum domain behaviour of classically chaotic systems can be studied through a causal interpretation of quantum mechanics. In this paper the nature of 'Bohmian trajectories' generated within the purview of the quantum theory of motion has been analysed. Phase space distance function and the associated KS entropy clearly reveal the difference between classically chaotic and integrable systems. Hénon–Heiles and Barbanis oscillators bear the signature of classical domain chaotic dynamics whereas harmonic and CTW systems show markedly different
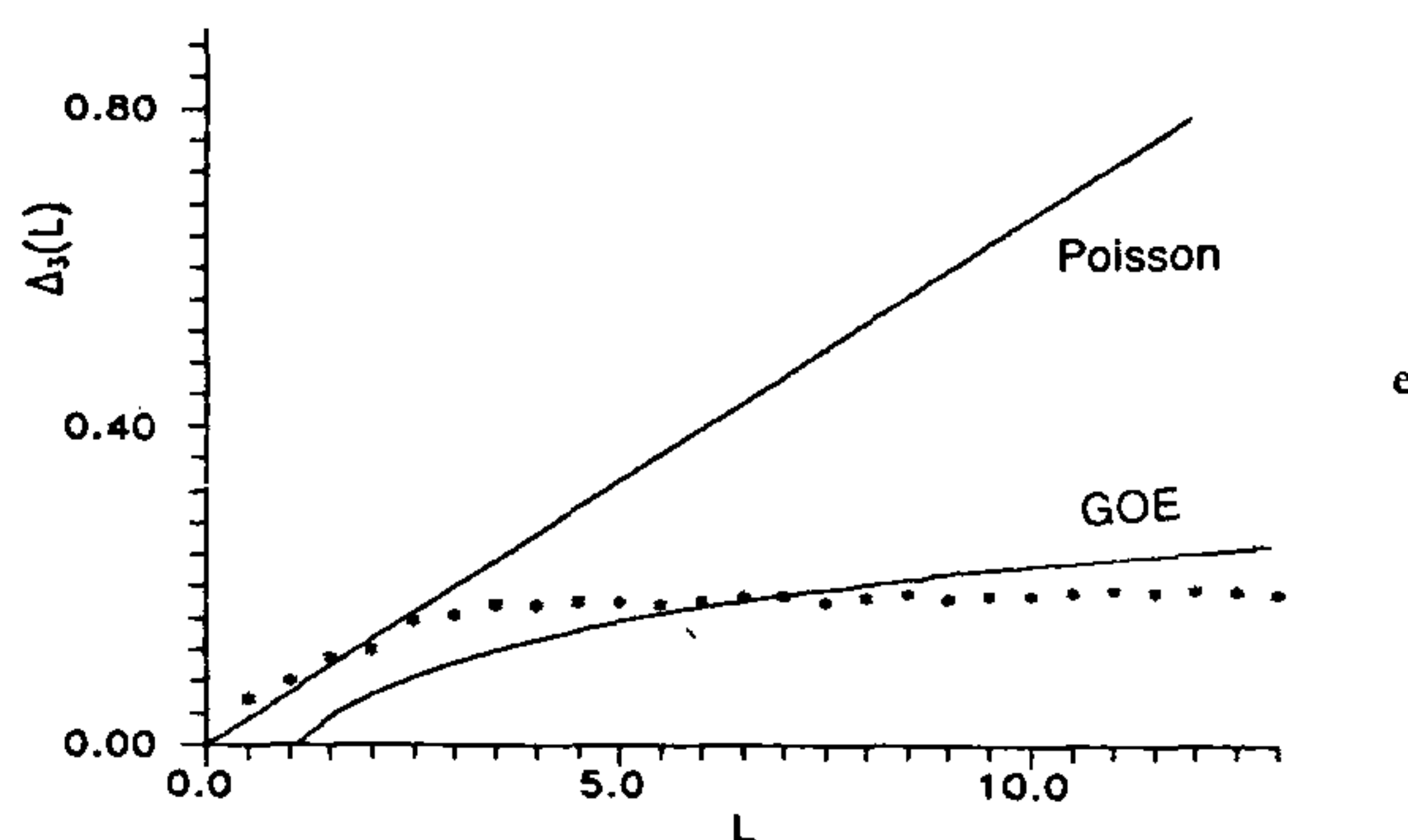
behaviour indicating the corresponding integrable nature. The QTM has reproduced the integrable nature of a quantum variant of the CTW system. Traditional measures of understanding 'quantum chaos', viz. autocorrelation function, power spectrum, phase space volume, nearest neighbour spacing distribution and spectral rigidity provide additional support towards identifying a classically chaotic system in the quantum domain.

1. Jensen R. V., Nature, 1995, 373, 16.
2. Eckhardt, B., Phys. Rep., 1988, 163, 205–297.
3. Gutzwiller, M. C., in Chaos in Classical and Quantum Mechanics, Springer, Berlin, 1990.
4. Reichl, L. E., in The Transition to Chaos in Conservative Classical Systems: Quantum Manifestations, Springer-Verlag, New York, 1992.
5. Casati, G., Chirikov, B. V., Guarneri, I. and Shepelyansky, D. L., Phys. Rep., 1987, 154, 77–123.
6. Feit, M. D. and Fleck, Jr. J. A., J. Chem. Phys., 1984, 80, 2578–2584.
7. Pomphrey, N., J. Phys. B., 1974, 7, 1909–1915.
8. Swimm, R. T. and Delos, J. B., J. Chem. Phys., 1979, 71, 1706–1717.
9. Noid, D. W., Koszykowski, M. L., Tabor, M. and Marcus, R. A., J. Chem. Phys., 1980, 72, 6169–6175.
10. Noid, D. W., Koszykowski, M. L. and Marcus, R. A., J. Chem. Phys., 1979, 71, 2864–2873.
11. Davis, M. J. and Heller, E. J., J. Chem. Phys., 1979, 71, 3383–3395.
12. Davis, M. J. and Heller, E. J., J. Chem. Phys., 1981, 75, 3916–3924.
13. Davis, M. J., Stechel, E. B. and Heller, E. J., Chem. Phys. Lett., 1980, 76, 21–26.
14. Nordholm, K. S. J. and Rice, S. A., J. Chem. Phys., 1974, 61, 203–223, 768–779.
15. Hutchinson, J. S. and Wyatt, R. E., Phys. Rev. A, 1981, 23, 1567–1584.
16. Chattaraj, P. K., Indian J. Pure. Appl. Phys., 1994, 32, 101–105.
17. Chattaraj, P. K. and Sengupta, S., Phys. Lett. A., 1993, 181, 225–231.
18. Chattaraj, P. K. and Sengupta, S., Indian J. Pure. Appl. Phys., 1996, 34, 518–527. There are some misprints in this paper.
19. Sengupta, S. and Chattaraj, P. K., Phys. Lett. A., 1996, 215, 119–227; Chattaraj, P. K., Sengupta, S. and Poddar, A., Int. J. Quantum Chem., DFT Spl. Issue, in press.
20. Brunner, P. and Shapiro, M., Chem. Phys. Lett., 1980, 72, 528–532.
21. Heller, E. J., J. Chem. Phys., 1978, 68, 2066.
22. Bixon, M. and Jortner, J., J. Chem. Phys., 1982, 77, 4175–4187.

23. Mahapatra, S. and Sathyamurthy, N., *J. Chem. Phys.*, 1995, **102**, 6057–6066; Mahapatra, S., Ramaswamy, R. and Sathyamurthy, N., *J. Chem. Phys.*, 1996, **104**, 1–9.

24. Nakamura, K. and Lakhshmanan, M., *Phys. Rev. Lett.*, 1986, **57**, 1661–1664.

25. Gespard, P., Rice, S. A. and Nakamura, K., *Phys. Rev. Lett.*, 1989, **63**, 930–933.

26. Contopoulos, G., *Bull. Astron.*, 1967, **2**, 223.

27. Chang, Y. F., Tabor, M. and Weiss, J., *J. Math. Phys.*, 1982, **23**, 531–538.

28. Mehta, M. L., in *Random Matrices and Statistical Theory of Energy Levels*, Academic Press, New York, 1965.

29. Dyson, F. J. and Mehta, M. L., *J. Math. Phys.*, 1963, **4**, 701–702.

30. Holland, P. R., in *The Quantum Theory of Motion*, Cambridge Univ. Press, Cambridge, 1993.

31. de Broglie, L., *C. R. Acad. Sci.*, 1926, **183**, 447–448; 1927, **184**, 273–274; 1927, **185**, 380–382.

32. Bohm, D., *Phys. Rev.*, 1952, **85**, 166–179, 180–193; in *Causality and Chance in Modern Physics*, Routledge and Kegan Paul, London, 1957.

33. Madelung, E., *Z. Phys.*, 1926, **40**, 332–326.

34. Schwengelbeck, U. and Faisal, F. H. M., *Phys. Lett. A*, 1995, **199**, 281–286.

35. Faisal, F. H. M. and Schwengelbeck, U., *Phys. Lett. A*, 1995, **207**, 31–36.

36. Chattaraj, P. K. and Sengupta, S., *Curr. Sci.*, 1996, **71**, 134–139.

37. Graham, R. and Hohnerbach, M., *Phys. Rev. A*, 1991, **43**, 3966–3981, *Phys. Rev. Lett.*, 1990, **64**, 637–640; Choudhury, S., Gangopadhayay, G. and Ray, D. S., *Indian J. Phys.*, 1995, **69B**, 507–523.

38. French, J. B. and Wong, S. S. M., *Nucl. Phys. A*, 1972, **198**, 188–208; Sinha, S. Ramaswamy, R., *Mol. Phys.*, 1989, **67**, 335.

39. Goldberg, A., Schey, H. M. and Schwartz, J. L., *Am. J. Phys.*, 1967, **35**, 177–186; *ibid*, 1968, **36**, 454–455; Galbraith, I., Ching, Y. S. and Abraham, E., *Am. J. Phys.*, 1984, **52**, 60–68.

40. Chattaraj, P. K., Rao, K. S. and Deb, B. M., *J. Comput. Phys.*, 1987, **72**, 504–512.

41. Berry, M. V. and Tabor, M., *Proc. R. Soc. London, Series A*, 1977, **356**, 375–394.